

# 2D–frequency domain identification of complex sinusoids in the presence of additive noise

Umberto Soverini \* Torsten Söderström \*\*

\* *Department of Electrical, Electronic and Information Engineering,  
University of Bologna, Italy  
(e-mail: umberto.soverini@unibo.it)*

\*\* *Department of Information Technology, Uppsala University, Sweden  
(e-mail: ts@it.uu.se)*

---

**Abstract:** This paper describes a new approach for identifying the parameters of two–dimensional complex sinusoids from a finite number of measurements, in presence of additive and uncorrelated two–dimensional white noise. The proposed approach is based on using frequency domain data. As a major feature, it enables the estimation to be frequency selective. The new method extends to the two–dimensional (2D) case some recent results obtained with reference to the frequency ESPRIT algorithm. The properties of the proposed method are analyzed by means of Monte Carlo simulations and its features are compared with those of a classical time domain estimation algorithm. The practical advantages of the method are highlighted. In fact the novel approach can operate just on a specified sub–area of the 2D spectrum. This area–selective feature allows a drastic reduction of the computational complexity, which is usually very high when standard time domain methods are used.

Keywords: System identification; Discrete Fourier Transform; 2D damped sinusoidal models.

---

## 1. INTRODUCTION

The two–dimensional (2D) spectral analysis is a well studied topic with a vast number of applications like, for example, image processing and 2D MR spectroscopy.

In the 2D spectral analysis literature (Marple, 1987; Kay, 1988) two different methodologies are usually described. The first one contains the classical nonparametric approaches, that suffer from several limitations such as poor resolution and high–sidelobe effects. The second methodology contains the parametric approaches. Nonparametric methods are usually developed in the frequency domain, while parametric methods treat time domain data.

Among the second class of methods, one can find the Maximum Likelihood method (Clark and Sharf, 1994) and the subspace–based approaches, like the harmonic retrieval method in (Kung et al., 1983), the MEMP method (Hua, 1992; Hua and Baqai, 1994; Zhu and Hua, 1993) and the ACMP method (Vanpoucke et al., 1994). Other approaches are the 2D–Prony method (Sacchini et al., 1993), the Linear Prediction method, see e.g. (Marple, 2000), the 2D–MODE algorithm (Li et al., 1996), the 2D–MUSIC method (Li et al., 1998) and the 2D–ESPRIT method (Rouquette and Najim, 2001; Wang et al., 2005).

The theoretical results provided by (Pintelon et al., 1997), with reference to input–output models, and by (McKelvey, 2000, 2002), for state–space models, have allowed to directly implement in the frequency domain many parametric approaches originally developed for time domain data (Pintelon and Schoukens, 2012).

Based on these results, in (Soverini and Söderström, 2017) a frequency subspace–based approach has been proposed for

the identification of one–dimensional complex sinusoids, in the presence of additive and uncorrelated white noise. The method can be considered as the frequency counterpart of the well–known ESPRIT method (Roy and Kailath, 1989), originally developed in the time domain. An alternative frequency domain approach was proposed also in (McKelvey and Viberg, 2001).

This paper extends the approach of (Soverini and Söderström, 2017) to the 2D case. It was originally motivated by the work of (Sandgren et al., 2006), where the ideas of (McKelvey and Viberg, 2001) have been applied in the 2D MR problems.

To the best of the authors’ knowledge, the obtained results about the 2D–DFT representation of 2D–dynamic systems constitute a novelty in the existing literature. In particular, they allow a rigorous definition of the identification problem, that can be directly formulated and solved in terms of the 2D–DFT data.

It must be observed that in many applications the data are directly available in the time domain and there is no practical need to perform the 2D–DFT before implementing the identification algorithm. On the other hand, the main purposes of this paper are to formulate and solve the identification problem in the frequency domain and to investigate the theoretical links among the time domain models and the corresponding frequency domain representations. For these reasons, as preliminary investigations, the comparison with other identification approaches existing in the literature has not been performed, with the exception of the method proposed in (Kung et al., 1983) since it constitutes the basis of the 2D time domain realization procedure.

As a major feature, working in the frequency domain enables the estimation to be frequency area–selective, i.e. the user has the possibility to take into account some *a priori* information,

by selecting the data just from the 2D frequency sub-bands in which the signal harmonics are known to reside.

The organization of the paper is as follows. Section 2 defines the problem of identifying 2D complex sinusoids buried in white measurement noise. Section 3 introduces a novel frequency domain description of the system model. In Sections 4 it is explained how the identification problem can be solved, by using the frequency domain subspace-based algorithm proposed in (Soverini and Söderström, 2017). In Section 5 the effectiveness of the proposed procedure is verified by means of Monte Carlo simulations and its features are compared with those of the 2D time domain method proposed in (Kung et al., 1983). It is shown that the proposed method exhibits very good performance and is characterized by high frequency resolution properties. Finally, some concluding remarks are reported in Section 6.

## 2. STATEMENT OF THE PROBLEM

Consider the following discrete time model for  $n$  2D complex sinusoids buried in measurement noise

$$x(t_1, t_2) = \sum_{i=1}^n \rho_i e^{\gamma_{1i} t_1} e^{\gamma_{2i} t_2} \quad (1)$$

$$y(t_1, t_2) = x(t_1, t_2) + v(t_1, t_2), \quad (2)$$

where  $t_1 = 0, \dots, N_1 - 1$ ,  $t_2 = 0, \dots, N_2 - 1$  and  $N_1, N_2$  denote the number of the available samples in each of the two dimensions.

The coefficients  $\gamma_{1i} = -\beta_{1i} + i\omega_{1i}$  and  $\gamma_{2i} = -\beta_{2i} + i\omega_{2i}$  contain the unknown damping and frequency parameters,  $\rho_i = |\rho_i|e^{i\varphi_i}$  are the unknown complex gains and  $v(t_1, t_2)$  is the complex 2D white noise.

The problem under consideration is to estimate the signal parameters  $\omega_{1i}, \beta_{1i}, \omega_{2i}, \beta_{2i}$  ( $i = 1, \dots, n$ ) and, possibly, the noise variance  $\sigma_v^*$ .

The following assumptions are applied.

- A1. The number  $n$  is *a priori* known and all the components are present,  $\rho_i \neq 0 \forall i$ .
- A2. The  $n$  frequencies are distinct in both directions, i.e.  $\omega_{1h} \neq \omega_{1l}$  and  $\omega_{2h} \neq \omega_{2l} \forall h, l, h \neq l$ , with  $\omega_{1h}, \omega_{2h} \in (-\pi, \pi]$ .
- A3. The additive noise  $v(t_1, t_2)$  is a 2D, zero-mean, complex-valued circular white noise, with *unknown* variance  $\sigma_v^*$  and is uncorrelated with  $x(t_1, t_2)$ .

Define  $\lambda_{1i} = e^{\gamma_{1i}}$  and  $\lambda_{2i} = e^{\gamma_{2i}}$  with  $i = 1, \dots, n$ .

It can be easily verified that  $(1 - \lambda_{1i} q_1^{-1})$  is an annihilating polynomial for the generic  $i$ -th signal  $x_i(t_1, t_2) = \rho_i e^{\gamma_{1i} t_1} e^{\gamma_{2i} t_2}$  in (1), i.e.

$$(1 - \lambda_{1i} q_1^{-1}) x_i(t_1, t_2) = 0, \quad (3)$$

where  $q_1^{-1}$  denotes the backward shift operator along the dimension  $t_1$ .

In an analogous way,  $(1 - \lambda_{2i} q_2^{-1})$  is an annihilating polynomial for the generic  $i$ -th signal  $x_i(t_1, t_2) = \rho_i e^{\gamma_{1i} t_1} e^{\gamma_{2i} t_2}$  in (1), i.e.

$$(1 - \lambda_{2i} q_2^{-1}) x_i(t_1, t_2) = 0, \quad (4)$$

where  $q_2^{-1}$  denotes the backward shift operator along the dimension  $t_2$ .

Relations (3)–(4) are direct consequences of the fact that  $x_i(t_1, t_2)$  is a separable signal in the two variables  $t_1$  and  $t_2$ . For (3)–(4) to hold for all time arguments, proper initial conditions must be set.

By extending this observation for all the components of  $x(t_1, t_2)$ , the following homogeneous AR equations can be obtained

$$A_1(q_1^{-1}) x(t_1, t_2) = 0 \quad (5)$$

$$A_2(q_2^{-1}) x(t_1, t_2) = 0, \quad (6)$$

where

$$\begin{aligned} A_1(z_1^{-1}) &= \prod_{i=1}^n (1 - \lambda_{1i} q_1^{-1}) \\ &= 1 + \alpha_{1,1} q_1^{-1} + \dots + \alpha_{1,n} q_1^{-n} \end{aligned} \quad (7)$$

$$\begin{aligned} A_2(q_2^{-1}) &= \prod_{i=1}^n (1 - \lambda_{2i} q_2^{-1}) \\ &= 1 + \alpha_{2,1} q_2^{-1} + \dots + \alpha_{2,n} q_2^{-n} \end{aligned} \quad (8)$$

and  $\alpha_{1,i}, \alpha_{2,i}$  ( $i = 1, \dots, n$ ) are complex parameters.

From (5)–(6) it follows that also

$$\begin{aligned} A(q_1^{-1}, q_2^{-1}) &= A_1(q_1^{-1}) A_2(q_2^{-1}) \\ &= \prod_{i=1}^n (1 - \lambda_{1i} q_1^{-1}) \prod_{i=1}^n (1 - \lambda_{2i} q_2^{-1}) \end{aligned} \quad (9)$$

is an annihilating polynomial for  $x(t_1, t_2)$ , i.e.

$$A(q_1^{-1}, q_2^{-1}) x(t_1, t_2) = 0. \quad (10)$$

For (10) to hold (for all time arguments) proper boundary conditions have to be set.

Equation (9) can be seen as a definition of  $A$ . It is worth observing that  $A(q_1^{-1}, q_2^{-1})$  is, by construction, a 2D separable polynomial in the two variables  $q_1^{-1}$  and  $q_2^{-1}$ .

We will face the identification problem in the frequency domain, using the Discrete Fourier Transform (DFT) of the signals. An exact description of the effects of the boundary conditions is given and exploited. Two ways are possible:

1. Formulate the problem using an input–output representation, i.e. starting from the difference equation (10), complemented with the effects of the boundary conditions. This is the approach taken in this paper.
2. Formulate the problem using a state space representation. Then, in a certain sense, initial conditions can be imposed instead of boundary conditions. This is the approach taken in (Soverini and Söderström, 2018).

As a main feature, for both papers the estimation procedure will work using only a subset of the 2D–frequency domain, that is part of the  $\omega_1, \omega_2$  space.

For a generic 1D signal  $\{s(t)\}_{t=0}^{N-1}$ , observed at  $N$  equidistant time instants, the one-dimensional Discrete Fourier Transform (1D–DFT) is defined as

$$S(\omega_h) = \frac{1}{\sqrt{N}} \sum_{t=0}^{N-1} s(t) e^{-i\omega_h t}, \quad (11)$$

where  $\omega_h = 2\pi h/N$ ,  $h = 0, \dots, N - 1$ .

It is well-known that the 1D–DFT defined in (11) admits also a matrix representation (see Appendix A).

For a generic 2D signal  $s(t_1, t_2)$  with  $t_1 = 0, \dots, N_1 - 1$ ,  $t_2 = 0, \dots, N_2 - 1$ , observed at equidistant time instants, the two-dimensional Discrete Fourier Transform (2D-DFT) is defined as

$$S(\omega_h, \omega_l) = \frac{1}{\sqrt{N_1 N_2}} \sum_{t_1=0}^{N_1-1} \sum_{t_2=0}^{N_2-1} s(t_1, t_2) e^{-i\omega_h t_1} e^{-i\omega_l t_2} \quad (12)$$

where  $\omega_h = 2\pi h/N_1$  ( $h = 0, \dots, N_1 - 1$ ) and  $\omega_l = 2\pi l/N_2$  ( $l = 0, \dots, N_2 - 1$ ).

By using the definition (11), the 2D-DFT (12) can be obtained in two steps, by computing the DFT with respect to  $t_1$ , keeping  $t_2$  fixed

$$\bar{S}_1(\omega_h, t_2) = \frac{1}{\sqrt{N_1}} \sum_{t_1=0}^{N_1-1} s(t_1, t_2) e^{-i\omega_h t_1} \quad (13)$$

and then computing the DFT of  $\bar{S}_1(\omega_h, t_2)$  with respect to  $t_2$

$$S(\omega_h, \omega_l) = \frac{1}{\sqrt{N_2}} \sum_{t_2=0}^{N_2-1} \bar{S}_1(\omega_h, t_2) e^{-i\omega_l t_2}. \quad (14)$$

Or *vice versa*, one can firstly proceed with respect to  $t_2$  and then with respect to  $t_1$

$$\bar{S}_2(t_1, \omega_l) = \frac{1}{\sqrt{N_2}} \sum_{t_2=0}^{N_2-1} s(t_1, t_2) e^{-i\omega_l t_2} \quad (15)$$

$$S(\omega_h, \omega_l) = \frac{1}{\sqrt{N_1}} \sum_{t_1=0}^{N_1-1} \bar{S}_2(t_1, \omega_l) e^{-i\omega_h t_1}. \quad (16)$$

It is worth observing that also the 2D-DFT defined in (12) can be expressed in matrix form (see Appendix A).

The problem under investigation can be stated as follows.

**Problem 1.** Let  $Y(\omega_h, \omega_l)$  ( $h = 0, \dots, N_1 - 1$ ;  $l = 0, \dots, N_2 - 1$ ) be the 2D-DFT of the noisy measurements  $y(t_1, t_2)$  generated by the system (1)–(2). Given  $Y(\omega_h, \omega_l)$ , estimate the signal parameters  $\omega_{1i}$ ,  $\beta_{1i}$ ,  $\omega_{2i}$ ,  $\beta_{2i}$  ( $i = 1, \dots, n$ ) and, possibly, the noise variance  $\sigma_v^*$ .

**Remark 1.** As pointed out in Problem 1, the main focus is on the non-linear problem of estimating the parameters  $\gamma_{1i} = -\beta_{1i} + i\omega_{1i}$  and  $\gamma_{2i} = -\beta_{2i} + i\omega_{2i}$ . Once the parameters  $\gamma_{1i}$  and  $\gamma_{2i}$  are known, in order to recover the model (1) it is necessary to develop a further procedure for pairing them properly  $\{\gamma_{1i}, \gamma_{2i}\}_{i=1}^n$  and for estimating the parameters  $\rho_i$ . This is a common aspect for many 2D methods, see e.g. (Hua, 1992). For this purpose, the procedure described in (Sandgren et al., 2006) can be applied. A brief summary can be found also in Appendix B of (Soverini and Söderström, 2018).  $\diamond$

### 3. FREQUENCY DOMAIN SET UP

In this section a new frequency domain description for the noisy model (1)–(2) is introduced.

Compute the 1D-DFT of equation (5) with respect to  $t_1$  for a fixed value of  $t_2$ , see definition (13). It is a well-known fact (Pintelon et al., 1997) that for finite  $N_1$ , even in absence of noise, the 1D-DFT  $\bar{X}_1(\omega_h, t_2)$  of the signal  $x(t_1, t_2)$  does no longer satisfy the relation (5). On the contrary, it exactly satisfies an extended relation that includes also a transient term

$$A_1(e^{-i\omega_h}) \bar{X}_1(\omega_h, t_2) = T_1(e^{-i\omega_h}, t_2), \quad (17)$$

where  $T_1(z_1^{-1}, t_2)$  is a polynomial of order  $n - 1$

$$T_1(z_1^{-1}, t_2) = \tau_{1,0}(t_2) + \tau_{1,1}(t_2) z_1^{-1} + \dots + \tau_{1,n-1}(t_2) z_1^{-n+1}. \quad (18)$$

Note that the polynomial in (18) is an explicit function of  $t_2$ , since changing  $t_2$  the values of the parameters  $\tau_{1,i}$  change. According to the theoretical results of the 1D case, the term  $T_1(e^{-i\omega_h}, t_2)$  is identically zero if  $x(t_1, t_2)$  is a  $N_1$ -periodic sequence in the  $t_1$  direction.

As before, it is possible to state that for finite  $N_2$ , even in absence of noise, the 1D-DFT  $\bar{X}_2(t_1, \omega_l)$  of the signal  $x(t_1, t_2)$  (see definition (15)) does no longer satisfy the relation (6). On the contrary, it exactly satisfies an extended relation that includes also a transient term

$$A_2(e^{-i\omega_l}) \bar{X}_2(t_1, \omega_l) = T_2(e^{-i\omega_l}, t_1), \quad (19)$$

where  $T_2(z_2^{-1}, t_1)$  is a polynomial of order  $n - 1$

$$T_2(z_2^{-1}, t_1) = \tau_{2,0}(t_1) + \tau_{2,1}(t_1) z_2^{-1} + \dots + \tau_{2,n-1}(t_1) z_2^{-n+1}. \quad (20)$$

The term  $T_2(e^{-i\omega_l}, t_1)$  is null if  $x(t_1, t_2)$  is a  $N_2$ -periodic sequence in the  $t_2$  direction.

According to (12), let  $X(\omega_h, \omega_l)$ ,  $Y(\omega_h, \omega_l)$  be the 2D-DFTs of the time domain sequences  $x(t_1, t_2)$  and  $y(t_1, t_2)$ , respectively.

Compute now the 1D-DFT on both sides of relation (17) with respect to  $t_2$ , according to relation (14). It results in

$$A_1(e^{-i\omega_h}) X(\omega_h, \omega_l) = \bar{T}_1(e^{-i\omega_h}, \omega_l), \quad (21)$$

where  $\bar{T}_1(z_1^{-1}, \omega_l)$  is the following polynomial of order  $n - 1$

$$\begin{aligned} \bar{T}_1(z_1^{-1}, \omega_l) &= \frac{1}{\sqrt{N_2}} \sum_{t_2=0}^{N_2-1} T_1(z_1^{-1}, t_2) e^{-i\omega_l t_2} \quad (22) \\ &= \left( \frac{1}{\sqrt{N_2}} \sum_{t_2=0}^{N_2-1} \tau_{1,0}(t_2) e^{-i\omega_l t_2} \right) \\ &+ \left( \frac{1}{\sqrt{N_2}} \sum_{t_2=0}^{N_2-1} \tau_{1,1}(t_2) e^{-i\omega_l t_2} \right) z_1^{-1} + \dots \\ &+ \left( \frac{1}{\sqrt{N_2}} \sum_{t_2=0}^{N_2-1} \tau_{1,n-1}(t_2) e^{-i\omega_l t_2} \right) z_1^{-n+1}. \quad (23) \end{aligned}$$

In other words, it results in

$$\bar{T}_1(z_1^{-1}, \omega_l) = \bar{\tau}_{1,0}(\omega_l) + \bar{\tau}_{1,1}(\omega_l) z_1^{-1} + \dots + \bar{\tau}_{1,n-1}(\omega_l) z_1^{-n+1} \quad (24)$$

where  $\bar{\tau}_{1,i}(\omega_l)$  are the 1D-DFTs of the sequences  $\tau_{1,i}(t_2)$

$$\bar{\tau}_{1,i}(\omega_l) = \frac{1}{\sqrt{N_2}} \sum_{t_2=0}^{N_2-1} \tau_{1,i}(t_2) e^{-i\omega_l t_2}, \quad (25)$$

for  $i = 0, \dots, n - 1$ . Note that the coefficients of  $\bar{T}_1(z_1^{-1}, \omega_l)$  are constant when  $\omega_l$  is fixed.

In a similar way, compute the 1D-DFT on both sides of relation (19) with respect to  $t_1$ , according to relation (16). It results in

$$A_2(e^{-i\omega_l}) X(\omega_h, \omega_l) = \bar{T}_2(e^{-i\omega_l}, \omega_h), \quad (26)$$

where  $\bar{T}_2(z_2^{-1}, \omega_h)$  is the following polynomial of order  $n - 1$

$$\begin{aligned} \bar{T}_2(z_2^{-1}, \omega_h) &= \bar{\tau}_{2,0}(\omega_h) + \bar{\tau}_{2,1}(\omega_h) z_2^{-1} + \dots \\ &+ \bar{\tau}_{2,n-1}(\omega_h) z_2^{-n+1} \quad (27) \end{aligned}$$

and  $\bar{\tau}_{2,i}(\omega_h)$  are the 1D-DFTs of the sequences  $\tau_{2,i}(t_1)$

$$\bar{\tau}_{2,i}(\omega_h) = \frac{1}{\sqrt{N_1}} \sum_{t_1=0}^{N_1-1} \tau_{2,i}(t_1) e^{-i\omega_h t_1}, \quad (28)$$

for  $i = 0, \dots, n - 1$ .

Summing up, the previous results can be formalized in the following theorem.

*Theorem 1.* Let  $X(\omega_h, \omega_l)$  be the 2D–DFT of the signal  $x(t_1, t_2)$ , generated by the 2D model (1), with finite values of  $N_1$  and  $N_2$ . The following relations hold exactly

$$A_1(e^{-i\omega_h}) X(\omega_h, \omega_l) = \bar{T}_1(e^{-i\omega_h}, \omega_l) \quad (29)$$

$$A_2(e^{-i\omega_l}) X(\omega_h, \omega_l) = \bar{T}_2(e^{-i\omega_l}, \omega_h), \quad (30)$$

where  $\bar{T}_1(z_1^{-1}, \omega_l)$  and  $\bar{T}_2(z_2^{-1}, \omega_h)$  are the polynomials defined in (24) and (27), respectively. The term  $\bar{T}_1(e^{-i\omega_h}, \omega_l)$  is null if  $X(\omega_h, \omega_l)$  is  $N_1$ –periodic with respect to  $\omega_h$ . Analogously, the term  $\bar{T}_2(e^{-i\omega_l}, \omega_h)$  is null if  $X(\omega_h, \omega_l)$  is  $N_2$ –periodic with respect to  $\omega_l$ .  $\diamond$

Recalling the result of (Pintelon et al., 1997), the extension to the frequency domain of the relation (10) can be stated as follows.

*Theorem 2.* For finite  $N_1$  and  $N_2$ , the 2D–DFT  $X(\omega_h, \omega_l)$  does no longer satisfy the relation (10). On the contrary, it exactly satisfies an extended relation that includes also a transient term

$$\begin{aligned} A(e^{-i\omega_h}, e^{-i\omega_l}) X(\omega_h, \omega_l) = \\ A_1(e^{-i\omega_h}) \bar{T}_2(e^{-i\omega_l}, \omega_h) = A_2(e^{-i\omega_l}) \bar{T}_1(e^{-i\omega_h}, \omega_l) = \\ \frac{1}{2} \left( A_1(e^{-i\omega_h}) \bar{T}_2(e^{-i\omega_l}, \omega_h) + A_2(e^{-i\omega_l}) \bar{T}_1(e^{-i\omega_h}, \omega_l) \right), \end{aligned} \quad (31)$$

where  $\bar{T}_1(z_1^{-1}, \omega_l)$  and  $\bar{T}_2(z_2^{-1}, \omega_h)$  have been defined in (24) and (27).  $\diamond$

*Proof.* By definition (9) of the polynomial  $A(z_1^{-1}, z_2^{-1})$ , equation (10) can be written as

$$A_1(z_1^{-1}) A_2(z_2^{-1}) x(t_1, t_2) = 0. \quad (32)$$

Consider the equation (29) and multiply both sides by the polynomial  $A_2(e^{-i\omega_l})$ . The following relation is obtained

$$\begin{aligned} A_1(e^{-i\omega_h}) A_2(e^{-i\omega_l}) X(\omega_h, \omega_l) = \\ A_2(e^{-i\omega_l}) \bar{T}_1(e^{-i\omega_h}, \omega_l). \end{aligned} \quad (33)$$

It can also be written as

$$A(e^{-i\omega_h}, e^{-i\omega_l}) X(\omega_h, \omega_l) = A_2(e^{-i\omega_l}) \bar{T}_1(e^{-i\omega_h}, \omega_l). \quad (34)$$

Consider now the equation (30) and multiply both sides by the polynomial  $A_1(e^{-i\omega_h})$ . The following relation is obtained

$$\begin{aligned} A_1(e^{-i\omega_h}) A_2(e^{-i\omega_l}) X(\omega_h, \omega_l) = \\ A_1(e^{-i\omega_h}) \bar{T}_2(e^{-i\omega_l}, \omega_h). \end{aligned} \quad (35)$$

It can also be written as

$$A(e^{-i\omega_h}, e^{-i\omega_l}) X(\omega_h, \omega_l) = A_1(e^{-i\omega_h}) \bar{T}_2(e^{-i\omega_l}, \omega_h). \quad (36)$$

By comparing (34) with (36), it results in

$$A_1(e^{-i\omega_h}) \bar{T}_2(e^{-i\omega_l}, \omega_h) = A_2(e^{-i\omega_l}) \bar{T}_1(e^{-i\omega_h}, \omega_l). \quad (37)$$

Finally, by summing the equations (34) and (36) one obtains the equation (31).  $\diamond$

#### 4. TWO–STEP SUBSPACE–BASED SOLUTION

In this section it is shown that, in order to solve Problem 1, the frequency domain procedure described in (Soverini and Söderström, 2017) can be applied twice.

Let  $\mathbf{X}$  and  $\mathbf{Y}$  be the 2D–DFT matrices with dimension  $N_1 \times N_2$  defined according to (A.7) and containing the entries  $X(\omega_h, \omega_l)$  and  $Y(\omega_h, \omega_l)$ , respectively.

Now introduce the notational convention that, for every fixed value of  $\omega_l$ , e.g.  $\omega_l = \bar{\omega}_l$ , the term  $X(\omega_h, \bar{\omega}_l)$  represent the  $l$ –th column of the matrix  $\mathbf{X}$ . Analogously, for every fixed  $\omega_h = \bar{\omega}_h$ , the term  $X(\bar{\omega}_h, \omega_l)$  represent the  $h$ –th row of  $\mathbf{X}$ . Analogous considerations hold for the noisy matrix  $\mathbf{Y}$ .

Define the following column vectors

$$\mathbf{x}_l^c(\omega_h) = X(\omega_h, \bar{\omega}_l) \quad (38)$$

$$\mathbf{x}_h^r(\omega_l) = X^T(\bar{\omega}_h, \omega_l), \quad (39)$$

introduce the following notations

$$T_{1l}(e^{-i\omega_h}) = \bar{T}_1(e^{-i\omega_h}, \bar{\omega}_l) \quad (40)$$

$$T_{2h}(e^{-i\omega_l}) = \bar{T}_2(e^{-i\omega_l}, \bar{\omega}_h) \quad (41)$$

and compute the following averages

$$\mathbf{x}^c(\omega_h) = \frac{1}{N_2} \sum_{l=0}^{N_2-1} \mathbf{x}_l^c(\omega_h) \quad (42)$$

$$\mathbf{x}^r(\omega_l) = \frac{1}{N_1} \sum_{h=0}^{N_1-1} \mathbf{x}_h^r(\omega_l) \quad (43)$$

$$T_1(e^{-i\omega_h}) = \frac{1}{N_2} \sum_{l=0}^{N_2-1} T_{1l}(e^{-i\omega_h}) \quad (44)$$

$$T_2(e^{-i\omega_l}) = \frac{1}{N_1} \sum_{h=0}^{N_1-1} T_{2h}(e^{-i\omega_l}). \quad (45)$$

Thanks to the linearity properties, it is easily seen from (29)–(30) that

$$A_1(e^{-i\omega_h}) \mathbf{x}^c(\omega_h) = T_1(e^{-i\omega_h}) \quad (46)$$

$$A_2(e^{-i\omega_l}) \mathbf{x}^r(\omega_l) = T_2(e^{-i\omega_l}). \quad (47)$$

Consider now the generic, discrete time 1D signal

$$x(t) = \sum_{i=1}^n \rho_i e^{\gamma_i t} \quad t = 0, \dots, N - 1 \quad (48)$$

$$y(t) = x(t) + v(t) \quad (49)$$

where  $v(t)$  is a zero–mean, complex–valued circular white noise, uncorrelated with  $x(t)$ . Let  $X(\omega_k)$ ,  $Y(\omega_k)$  and  $V(\omega_k)$  be the 1D–DFTs of  $x(t)$ ,  $y(t)$  and  $v(t)$  respectively. For the noise–free data  $X(\omega_k)$ , define the polynomials

$$A(z^{-1}) = 1 + \alpha_1 z^{-1} + \dots + \alpha_n z^{-n} \quad (50)$$

$$T(z^{-1}) = \tau_0 + \tau_1 z^{-1} + \dots + \tau_{n-1} z^{-n+1}, \quad (51)$$

where  $z^{-1}$  denotes the backward shift operator, and write the following set of equations

$$A(e^{-i\omega_k}) X(\omega_k) = T(e^{-i\omega_k}), \quad (52)$$

with  $k = 0, \dots, N - 1$ .

Note that relation (46) is obtained from (52) if the following substitutions are introduced

$$\omega_k = \omega_h \quad N = N_1 \quad X(\omega_k) = \mathbf{x}^c(\omega_h)$$

$$A(z^{-1}) = A_1(z_1^{-1}) \quad T(z^{-1}) = T_1(z_1^{-1}).$$

In analogous way, it can be easily verified that (47) is obtained from (52) by making the following substitutions

$$\omega_k = \omega_l \quad N = N_2 \quad X(\omega_k) = \mathbf{x}^r(\omega_l)$$

$$A(z^{-1}) = A_2(z_2^{-1}) \quad T(z^{-1}) = T_2(z_2^{-1}).$$

With these definitions, the same notations used in (Soverini and Söderström, 2017) have been introduced, see also Appendix B. In the present case, the method is applied twice to the noisy data  $Y(\omega_k) = X(\omega_k) + V(\omega_k)$ , as follows.

Starting from the knowledge of the 2D-DFT noisy matrix  $\mathbf{Y}$ , the solution of Problem 1 can be obtained with the following two step procedure, that will be denoted as 2D–FD–ESPRIT method since it can be considered the 2D version of the FD–ESPRIT method of (Soverini and Söderström, 2017).

*Procedure 1.* As a first step, the identification procedure described in Appendix B can be applied to the vector  $\mathbf{y}^c(\omega_h)$ , obtained as in (42) by averaging over the columns  $\mathbf{y}_l^c(\omega_h) = Y(\omega_h, \bar{\omega}_l)$  of the matrix  $\mathbf{Y}$ . The procedure leads to the determination of the parameters  $\gamma_{1i} = -\beta_{1i} + i\omega_{1i}$ , with  $i = 1, \dots, n$ . Then, in a second step, the same identification procedure can be applied to the vector  $\mathbf{y}^r(\omega_l)$ , obtained as in (43) by averaging over the rows  $\mathbf{y}_h^r(\omega_l) = Y^T(\bar{\omega}_h, \omega_l)$  of the matrix  $\mathbf{Y}$ . The procedure leads to the determination of the parameters  $\gamma_{2i} = -\beta_{2i} + i\omega_{2i}$ , with  $i = 1, \dots, n$ .  $\diamond$

From simulation experiences, the effect of the additive noise is reduced and better parameter estimates are obtained by improving the Procedure 1 as follows. The procedure will be denoted as 2D–FD–ESPRIT–ENH(anced) method.

*Procedure 2.* As a first step, for each value of  $l$ , the identification procedure described in Appendix B is applied to the vectors  $\mathbf{y}_l^c(\omega_h) = Y(\omega_h, \bar{\omega}_l)$  of  $\mathbf{Y}$ . Thus, for each value of  $l$ , a matrix  $\Sigma_l$  of type (B.9) is obtained. Finally, the singular value decomposition (B.10) is performed on the matrix  $\Sigma$  obtained by averaging over the matrices  $\Sigma_l$ , with  $l \in [0, N_2 - 1]$ . The procedure leads to the determination of the parameters  $\gamma_{1i} = -\beta_{1i} + i\omega_{1i}$ , with  $i = 1, \dots, n$ .

Then, in a second step, the same identification procedure can be applied to each vector  $\mathbf{y}_h^r(\omega_l) = Y^T(\bar{\omega}_h, \omega_l)$  of  $\mathbf{Y}$ . Thus, for each value of  $h$ , a matrix  $\Sigma_h$  of type (B.9) is obtained. Finally, the singular value decomposition (B.10) is performed on the matrix  $\Sigma$  obtained by averaging over the matrices  $\Sigma_h$ , with  $h \in [0, N_1 - 1]$ . The procedure leads to the determination of the parameters  $\gamma_{2i} = -\beta_{2i} + i\omega_{2i}$ , with  $i = 1, \dots, n$ .  $\diamond$

*Remark 2.* Both steps of the Procedures 1 and 2 can be applied also when only a subset of the whole frequency range is used, i.e.  $\omega_h \in W_1 = [\omega_{I_1}, \omega_{F_1}]$ , with  $I_1 \geq 0$  and  $F_1 \leq N_1 - 1$ ; and  $\omega_l \in W_2 = [\omega_{I_2}, \omega_{F_2}]$ , with  $I_2 \geq 0$  and  $F_2 \leq N_2 - 1$ , on condition that the number of frequencies  $L_1 = F_1 - I_1 + 1$  and  $L_2 = F_2 - I_2 + 1$  is large enough. The subset  $W = W_1 \times W_2$  must be chosen by the user on the basis of *a priori* knowledge of the complex signal  $x(t_1, t_2)$  and allows a frequency area-selective estimate of the model parameters.  $\diamond$

*Remark 3.* After these two steps, in order to recover the original signal (1), the parameters  $\gamma_{1i}, \gamma_{2i}$  must be properly paired and the estimates of the parameters  $\rho_i$  must be computed. As stated in Remark 1, both operations can be performed simultaneously by using the procedure described in (Sandgren et al., 2006).  $\diamond$

## 5. NUMERICAL EXAMPLES

In this section, the effectiveness of the proposed 2D–FD–ESPRIT–ENH method is tested by means of numerical simulations. Its performance is compared with a revised version of the 2D time domain realization procedure, originally proposed in (Kung et al., 1983). A brief description of this procedure,

Table 1. System parameters

	$\omega_{1i}$	$\omega_{2i}$	$\beta_{1i}$	$\beta_{2i}$	$\rho_i$
$i = 1$	0.200	-0.010	0.06	0.06	$70 e^{0.5\pi}$
$i = 2$	-0.225	0.185	0.07	0.08	$100 e^{0.5\pi}$
$i = 3$	-0.210	0.200	0.07	0.09	$100 e^{0.5\pi}$
$i = 4$	0.050	-0.060	0.13	0.09	$120 e^{0.5\pi}$
$i = 5$	0.060	0.320	0.21	0.29	$400 e^{0.5\pi}$

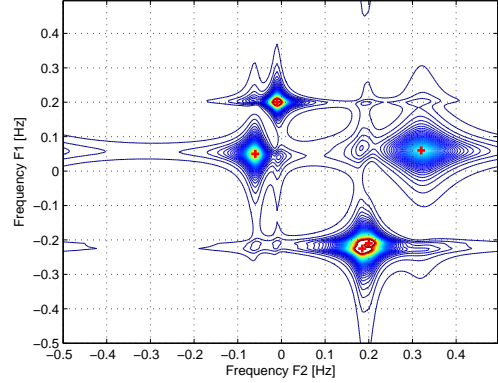


Fig. 1. Contour plot of the 2D–DFT spectrum.

denoted for convenience 2D–TD–KUNG method, can be found in Appendix A of (Soverini and Söderström, 2018).

*Example 1.* The following example has been proposed in (Sandgren et al., 2006) and mimics a Magnetic Resonance data analysis. The simulated system of type (1)–(2) consists of  $n = 5$  components. The true frequency and damping parameters are reported in Table 1, together with the complex gains (not estimated).

The number of samples of the considered data matrix is  $N_1 = 200$ ,  $N_2 = 200$  and the sampling frequency is  $f_s = 1$  Hz, so that the frequency resolution results in  $df = f_s/N = 0.005$  Hz. The contour plot of the 2D–DFT spectrum is shown in Fig. 1.

A Monte Carlo simulation of 100 independent runs has been performed by adding to the noise-free sequences  $x(t)$  different circular white noise realizations with variance  $\sigma_v^* = 6.7788$ , corresponding to a Signal to Noise Ratio (SNR) of 30 dB.

Table 2 reports the empirical means of the estimates of the system parameters  $\omega_{1i}, \omega_{2i}, \beta_{1i}$  and  $\beta_{2i}$  ( $i = 1, \dots, 5$ ), together with the corresponding standard deviations, obtained with the proposed 2D–FD–ESPRIT–ENH algorithm. The table reports also the results obtained with the time domain 2D–TD–KUNG algorithm. For both methods the order  $m > n$  of the augmented model (see step 3 in Appendix B) has been fixed to  $m = 66$ .

Table 2 shows that both identification methods yield similar, very good results. For lower SNR conditions the 2D–FD–ESPRIT–ENH algorithm does not yield good estimates. However, good results can be obtained by a proper selection of the 2D frequency sub-area  $W_1 \times W_2$  of the spectrum. On the basis of *a priori* knowledge, the frequency sub-area must be chosen in such a way to isolate the peaks under study, reducing the effects of the other neighbor peaks as much as possible.

Table 2. Estimated values of the parameters  $\omega_{1i}, \omega_{2i}, \beta_{1i}$  and  $\beta_{2i}$  – SNR=30 dB

	2D – FD – ESPRIT – ENH				2D – TD – KUNG			
	$\omega_{1i}$	$\omega_{2i}$	$\beta_{1i}$	$\beta_{2i}$	$\omega_{1i}$	$\omega_{2i}$	$\beta_{1i}$	$\beta_{2i}$
$i = 1$	$0.2000 \pm 0.0001$	$-0.0100 \pm 0.0001$	$0.0601 \pm 0.0004$	$0.0600 \pm 0.0004$	$0.1999 \pm 0.0001$	$-0.0100 \pm 0.0001$	$0.0606 \pm 0.0006$	$0.0607 \pm 0.0006$
$i = 2$	$-0.2250 \pm 0.0002$	$0.1850 \pm 0.0003$	$0.0702 \pm 0.0012$	$0.0800 \pm 0.0018$	$-0.2248 \pm 0.0003$	$0.1852 \pm 0.0003$	$0.0695 \pm 0.0021$	$0.0790 \pm 0.0024$
$i = 3$	$-0.2100 \pm 0.0002$	$0.1999 \pm 0.0004$	$0.0699 \pm 0.0014$	$0.0899 \pm 0.0023$	$-0.2102 \pm 0.0004$	$0.1997 \pm 0.0004$	$0.0707 \pm 0.0025$	$0.0908 \pm 0.0026$
$i = 4$	$0.0502 \pm 0.0008$	$-0.0600 \pm 0.0001$	$0.1287 \pm 0.0043$	$0.0899 \pm 0.0007$	$0.0503 \pm 0.0007$	$-0.0590 \pm 0.0007$	$0.1240 \pm 0.0036$	$0.0892 \pm 0.0041$
$i = 5$	$0.0601 \pm 0.0007$	$0.3200 \pm 0.0002$	$0.2083 \pm 0.0040$	$0.2899 \pm 0.0013$	$0.0591 \pm 0.0007$	$0.3188 \pm 0.0010$	$0.2137 \pm 0.0046$	$0.2948 \pm 0.0071$

Table 3. Estimated values of the parameters  $\omega_{1i}$  and  $\omega_{2i}$  – SNR=10 dB

	$\omega_{1i}$	$\omega_{2i}$	$W_1 \times W_2$
$i = 1$	$0.1898 \pm 0.0052$	$-0.0084 \pm 0.0010$	$[0.1, 0.3] \times [0.0, 1.0]$
$i = 2$	$-0.2312 \pm 0.0056$	$0.1560 \pm 0.0029$	$[0.7, 0.9] \times [0.1, 0.3]$
$i = 3$	$-0.1775 \pm 0.0040$	$0.2285 \pm 0.0043$	
$i = 4$	$0.0477 \pm 0.0016$	$-0.0554 \pm 0.0018$	$[0, 0.1] \times [0.9, 1]$
$i = 5$	$0.0476 \pm 0.0015$	$0.3226 \pm 0.0029$	$[0, 0.1] \times [0.25, 0.4]$

Table 3 reports the empirical means of the estimates and the corresponding standard deviations for the frequencies  $\omega_{1i}$  and  $\omega_{2i}$ , obtained in a Monte Carlo simulation of 100 independent runs with a SNR of 10 dB. Under these low SNR conditions the 2D–TD–KUNG algorithm fails to give correct results. The last column of Table 3 reports the frequency sub–band  $W_1 \times W_2$  (in Hz) used for the identification of the  $i$ -th 2D frequency. Two facts are worth observing. The same sub–area has been used for the joined estimate of the two peaks ( $\omega_{12}, \omega_{22}$ ) and ( $\omega_{13}, \omega_{23}$ ), in other words the number of 2D sinusoids to be identified in that area has been fixed to  $n = 2$ . The algorithm has some difficulties in discriminating the frequencies  $\omega_{14} = 0.050$  and  $\omega_{15} = 0.060$  along the  $t_1$  axis. Good estimates of the two peaks ( $\omega_{14}, \omega_{24}$ ) and ( $\omega_{15}, \omega_{25}$ ) have been obtained by using two disjoint sub–areas.

## 6. CONCLUSIONS

In this paper a novel 2D–frequency subspace–based approach has been proposed for the identification of complex–valued sinusoids affected by additive white noise. Its estimation properties have been tested and compared with a classical time domain technique by means of Monte Carlo simulations. The numerical results have confirmed the good performance of the new method.

### Appendix A. DFT MATRIX REPRESENTATION

Consider the  $N \times N$  Fourier matrix  $F_N$  whose entries are defined as follows

$$F_N = [f_{jk}] \quad (\text{A.1})$$

$$f_{jk} = \frac{1}{\sqrt{N}} e^{-i \frac{2\pi}{N} (j-1)(k-1)} \quad j, k = 1, \dots, N. \quad (\text{A.2})$$

It can be shown that  $F_N$  is a symmetric unitary matrix, and thus  $F_N = F_N^T = F_N^H$ .

Defining the following vectors in time and frequency domain

$$s = [s(0) \dots s(N-1)]^T \quad (\text{A.3})$$

$$S = [S(\omega_0) \dots S(\omega_{N-1})]^T \quad (\text{A.4})$$

the relation (11) can be represented by the linear transformation

$$S = F_N s. \quad (\text{A.5})$$

For the 2D case, denote with  $F_{N_1}$  and  $F_{N_2}$  the Fourier matrices of type (A.1)–(A.2) with dimension  $N_1 \times N_1$  and  $N_2 \times N_2$ , respectively. Define the following matrices containing the 2D time and frequency domain data

$$s = \begin{bmatrix} s(0,0) & s(0,1) & \dots & s(0,N_2-1) \\ s(1,0) & s(1,1) & \dots & s(1,N_2-1) \\ \vdots & \vdots & \ddots & \vdots \\ s(N_1-1,0) & s(N_1-1,1) & \dots & s(N_1-1,N_2-1) \end{bmatrix} \quad (\text{A.6})$$

$$S = \begin{bmatrix} S(\omega_0, \omega_0) & S(\omega_0, \omega_1) & \dots & S(\omega_0, \omega_{N_2-1}) \\ S(\omega_1, \omega_0) & S(\omega_1, \omega_1) & \dots & S(\omega_1, \omega_{N_2-1}) \\ \vdots & \vdots & \ddots & \vdots \\ S(\omega_{N_1-1}, \omega_0) & S(\omega_{N_1-1}, \omega_1) & \dots & S(\omega_{N_1-1}, \omega_{N_2-1}) \end{bmatrix}. \quad (\text{A.7})$$

Observe that in equation (13) the summation is with respect to the row index  $t_1$  while the column index  $t_2$  is fix. This expression can be considered as a 1D–DFT on the  $N_2$  columns of matrix (A.6). Thus, the equation (13) can be expressed in the matrix form

$$S_{\omega,t} = F_{N_1} s, \quad (\text{A.8})$$

where matrix  $S_{\omega,t}$  contains the elements  $S(\omega_h, t_2)$

$$S_{\omega,t} = \begin{bmatrix} S(\omega_0,0) & S(\omega_0,1) & \dots & S(\omega_0,N_2-1) \\ S(\omega_1,0) & S(\omega_1,1) & \dots & S(\omega_1,N_2-1) \\ \vdots & \vdots & \ddots & \vdots \\ S(\omega_{N_1-1},0) & S(\omega_{N_1-1},1) & \dots & S(\omega_{N_1-1},N_2-1) \end{bmatrix}. \quad (\text{A.9})$$

It can also be observed that in equation (14) the summation is with respect to the column index  $t_2$  while the row index  $\omega_h$  is fix. This expression can be considered as a 1D–DFT on the  $N_1$  rows of matrix (A.9) or, equivalently, on the  $N_1$  columns of matrix  $S_{\omega,t}^T$ . Thus, the equation (14) can be expressed in the following matrix form

$$S^T = F_{N_2} S_{\omega,t}^T. \quad (\text{A.10})$$

The resulting matrix is the transpose of the matrix  $S$  defined in (A.7). Thus, it results in

$$S = S_{\omega,t} F_{N_2}^T \quad (\text{A.11})$$

Recalling the properties of  $F_N$ , from (A.8) and (A.11) one finally obtains

$$S = F_{N_1} s F_{N_2} \quad (\text{A.12})$$

and *vice versa*

$$s = F_{N_1}^H S F_{N_2}^H. \quad (\text{A.13})$$

### Appendix B. THE 1D–FD–ESPRIT METHOD

In this appendix the 1D–frequency domain, subspace–based identification procedure described in (Soverini and Söderström,

2017) is briefly summarized. The method makes use of the state–space representation of the 1D model (48)–(49).

- (1) Compute the DFT  $Y(\omega_k)$  of the time domain data  $y(t)$ , generated by the  $n$ –order model (48)–(49).

- (2) Construct the  $N \times N$  diagonal matrix

$$V_Y^{diag} = \text{diag}[Y(\omega_0), Y(\omega_1), \dots, Y(\omega_{N-1})]. \quad (\text{B.1})$$

- (3) Select an appropriate integer  $m > n$  (a user choice).

- (4) Define the row vectors

$$\Omega_{m+1}(\omega_k) = [1 \ e^{-j\omega_k} \ \dots \ e^{-j(m-1)\omega_k} \ e^{-jm\omega_k}] \quad (\text{B.2})$$

$$\Omega_m(\omega_k) = [1 \ e^{-j\omega_k} \ \dots \ e^{-j(m-1)\omega_k}] \quad (\text{B.3})$$

and construct the matrices

$$\Psi_{m+1} = \begin{bmatrix} \Omega_{m+1}(\omega_0) \\ \vdots \\ \Omega_{m+1}(\omega_{N-1}) \end{bmatrix} \quad \Psi_m = \begin{bmatrix} \Omega_m(\omega_0) \\ \vdots \\ \Omega_m(\omega_{N-1}) \end{bmatrix} \quad (\text{B.4})$$

of dimension  $N \times (m+1)$  and  $N \times m$ , respectively.

- (5) Compute the matrix

$$\Pi_Y = V_Y^{diag} \Psi_{m+1} \quad (\text{B.5})$$

and construct the  $N \times (2m+1)$  matrix

$$\Phi_Y = [\Pi_Y \mid \Psi_m]. \quad (\text{B.6})$$

- (6) Compute the  $(2m+1) \times (2m+1)$  positive definite matrix

$$\Sigma_Y = \frac{1}{N} (\Phi_Y^H \Phi_Y). \quad (\text{B.7})$$

- (7) Partition matrix  $\Sigma_Y$  as follows

$$\Sigma_Y = \begin{bmatrix} \Sigma_{11} & \Sigma_{12} \\ \Sigma_{21} & \Sigma_{22} \end{bmatrix}, \quad (\text{B.8})$$

where  $\Sigma_{11}$  and  $\Sigma_{22}$  are square matrices with dimensions  $m+1$  and  $m$ , respectively.

- (8) Compute the  $(m+1) \times (m+1)$  matrix

$$\Sigma = \Sigma_{11} - \Sigma_{12} \Sigma_{22}^{-1} \Sigma_{21}. \quad (\text{B.9})$$

- (9) Compute the singular value decomposition

$$\Sigma = U \Lambda U^H \quad (\text{B.10})$$

and proceed with the classical ESPRIT algorithm (Roy and Kailath, 1989). See also, for example, Section 5 in (Soverini and Söderström, 2017).

## REFERENCES

- Clark, M.P. and Sharf, L.L. (1994). Two–dimensional modal analysis based on maximum likelihood. *IEEE Transactions on Signal Processing*, 42(6), 1443–1452.
- Hua, Y. (1992). Estimating two–dimensional frequencies by matrix enhancement and matrix pencil. *IEEE Transactions on Signal Processing*, 40, 2267–2280.
- Hua, Y. and Baqai, F. (1994). Correction to: Estimating two–dimensional frequencies by matrix enhancement and matrix pencil. *IEEE Transactions on Signal Processing*, 42, 1288.
- Kay, S. M. (1988). *Modern Spectral Estimation*, Prentice–Hall, Englewood Cliffs, New Jersey.
- Kung, S.Y., Arun, K.S. and Bhaskar Rao, D.V. (1983). State–space and singular value decomposition–based approximation methods for harmonic retrieval problem. *Journal of Optical Society of America*, 73(12), 1799–1811.
- Li, Y., Razavilar, J. and Ray Liu, K.J. (1998). A high–resolution technique for multidimensional NMR spectroscopy. *IEEE Transactions on Biomedical Engineering*, 45, 78–86.
- Li, J., Stoica, P. and Zheng, D. (1996). An efficient algorithm for two–dimensional frequency estimation. *Multidimensional Systems and Signal Processing*, 7, 151–178.
- Marple, L. (1987). *Digital Spectral Analysis with Applications*, Prentice–Hall, Englewood Cliffs, New Jersey.
- Marple, L. (2000). Two–dimensional lattice linear prediction parameter estimation method and fast algorithm. *IEEE Signal Processing Letters*, 7(6), 164–168.
- McKelvey, T. (2000). Frequency domain identification. *Proc. of the 12th IFAC Symposium on System Identification*, Plenary Paper. Santa Barbara, California USA.
- McKelvey, T. (2002). Frequency domain identification methods. *Circuits Systems Signal Processing*, 21(1), 39–55.
- McKelvey, T. and Viberg, M. (2001). A robust frequency domain subspace algorithm for multi–component harmonic retrieval. *Proc. of the 35th Asilomar Conference on Signals, Systems and Computers*, Pacific Grove, CA, 1288–1292.
- Pintelon, R. and Schoukens, J. (2012). *System identification: a frequency domain approach* (2nd ed.). NY: IEEE Press.
- Pintelon, R., Schoukens, J. and Vandersteen G. (1997). Frequency domain system identification using arbitrary signals. *IEEE Transactions on Automatic Control*, 42, 1717–1720.
- Rouquette, S. and Najim, M. (2001). Estimation of frequencies and damping factors by two–dimensional ESPRIT methods. *IEEE Transactions on Signal Processing*, 49, 237–245.
- Roy, R. and Kailath, T. (1989). ESPRIT–Estimation of signal parameters via rotational invariance techniques. *IEEE Transactions on Acoustics, Speech and Signal Processing*, 37, 984–995.
- Sandgren, N., Stoica, P. and Frigo, F.J. (2006). Area–selective signal parameter estimation for two–dimensional MR spectroscopy data. *Journal of Magnetic Resonance*, 183, 50–59.
- Sacchini, J.J., Steedy, W.M. and Moses, R.L. (1993). Two–dimensional Prony modeling and parameter estimation. *IEEE Transactions on Signal Processing*, 41, 3127–3136.
- Soverini, U. and Söderström, T. (2017). Frequency domain identification of complex sinusoids in the presence of additive noise. *Proc. of the 20–th IFAC World Conference*, Toulouse, France, 6418–6424.
- Soverini, U. and Söderström, T. (2018). Identification of two–dimensional complex sinusoids in white noise: a frequency domain approach. Submitted for presentation at the *18–th IFAC SYSID*, Stockholm, Sweden.
- Vanpoucke, F., M.Moonen, Y. and Berthoumieu, Y. (1994). An efficient subspace algorithm for 2–D harmonic retrieval. *Proc. of ICASSP*, Adelaide, Australia, 461–464.
- Wang, Y., Chen J.W. and Liu, Z. (2005). Comments on: Estimation of frequencies and damping factors by two–dimensional ESPRIT methods. *IEEE Transactions on Signal Processing*, 53.
- Zhu, Y. and Hua, Y. (1993). Spectral estimation of two–dimensional NMR signals by matrix pencil method. *Proc. Comp. Commun. Control Power Eng*, 3, 546–549.